Published in final edited form as:
J Neurochem. 2009 February ; 108(3): 835–846. doi:10.1111/j.1471-4159.2008.05838.x.

DIDS protects against neuronal injury by blocking Toll-like receptor 2 activated-mechanisms

Hang Yao[1], **Hady Felfly**[1], **Juan Wang**[1], **Dan Zhou**[1], and **Gabriel G Haddad**[1,2,3]

[1]Department of Pediatrics (Section of Respiratory Medicine), University of California San Diego, La Jolla, CA 92093

[2]Department of Neuroscience, University of California San Diego, La Jolla, CA 92093

[3]Rady Children's Hospital-San Diego, San Diego, CA 92123

Abstract

Using an in vitro ischemia model (ischemic solution, IS model) that induces penumbral cell death, we examined the effect of 4,4'-diisothio-cyanostilbene-2,2'-disulfonic acid (DIDS) on cell injury/death and underlying molecular mechanisms. Propidium iodide (PI) uptake was used to quantify cell death in organotypic hippocampal slice cultures. A 24-hr IS exposure caused a 5-fold increase in mean PI fluorescence intensity. DIDS, dose-dependently (1–4000 μM), reduced the IS-induced PI uptake in hippocampal CA1 neurons with an IC_{50} of 26 μM. This protective effect of DIDS was reversible and effective even 6 hrs following the onset of IS treatment. Gene expression profiling studies indicated that among ~46,000 transcripts tested, the most significantly up-regulated gene by IS was interleukin-1β (IL-1β) which was also the most significantly down-regulated gene when DIDS was added to the IS-treated slices. The addition of a recombinant interleukin-1 receptor antagonist (100μg/ml) or neutralizing IL-1β antibody significantly attenuated the IS-induced cell death, indicating that the up-regulation of IL-1β with IS treatment contributed to the IS-induced cell death. Toll-like receptor 2 (TLR2), another gene that was significantly up-regulated by IS and suppressed by DIDS, was studied to determine whether it was related to the IL-1β up-regulation. Indeed, this was the case as the IS-induced IL-1β up-regulation was abolished in $TLR2^{-/-}$ mouse brain slices. Furthermore, the IS-induced cell death was significantly reduced in $TLR2^{-/-}$ when compared with that in WT slices, indicating that TLR2 is functionally upstream of IL-1β in this IS model. We conclude that a) IS up-regulates TLR2 expression and augments TLR2 signaling, causing overexpression of IL-1β which leads to cell death; b) DIDS blocks IS-induced neuronal injury, at least partially, by suppressing the TLR2 pathway.

Introduction

One of the clinically important aspects of the pathobiology of cerebral ischemic infarcts (focal ischemia) is that these infarcts expand and worsen neurologic outcomes. Indeed, previous studies have demonstrated that this expansion occurs in both stroke patients and experimental animal models (Fisher 2006). Histopathological studies from a rat middle cerebral artery occlusion model have demonstrated that the ischemic area appearing as small lesions in the preoptic area within 30 minutes enlarges to involve the striatum and, at a later stage, involves even the cerebral cortex (Garcia et al. 1993). Similar observations have been made in human stroke patients using neuroimaging approaches (Baird et al. 1997; Karonen

Corresponding author: Gabriel G. Haddad, M.D., Department of Pediatrics, University of California San Diego, 9500 Gilman Drive, Dept. 0735, La Jolla, CA 92093-0735, Phone: 858-822-4740, 858-966-8536, Fax: 858-534-6972, E-mail: ghaddad@ucsd.edu.

et al. 1999; Parsons et al. 2002). About 38% to 156% infarct growth was estimated in stroke patients by the 'mismatch' of perfusion and diffusion on MRI (Back et al. 2004).

Human pathology and animal stroke model studies have shown that the ischemic infarcts grow at the expense of salvageable penumbral tissues. Previous reports have suggested that cell death in the penumbral tissue is associated with change in gene expression and apoptosis (Sharp et al. 2000; Lo et al. 2005). The delay in penumbral cell death provides a window of opportunity for clinical intervention. Evidence has been accumulating to demonstrate that the outcome of thrombolysis is closely related to the rescue of penumbral tissues (Gonzalez 2006). Therefore, preserving penumbral tissue is of paramount importance and is critical for improving stroke therapy (Fisher and Ratan 2003). However, mechanisms of cell death in the ischemic penumbral tissues are largely unknown.

In order to mimic the pathophysiology in the ischemic penumbra, we have recently developed in our laboratory an in vitro model consisting of organotypic brain slice cultures and an "ischemic solution" (IS) which is characterized by low O_2, low glucose, low pH, excitotoxic levels of glutamate and ionic alterations (Yao et al. 2007a). With this model, we have demonstrated that cell injury/death occurs in hippocampal slices subjected to IS. When we investigated in this model the role of major factors in cell injury, we showed that the alterations of four major ionic species, namely, K^+, Na^+ Ca^{2+} and Cl^- are of critical importance. For example, restoring extracellular Cl^- concentration to physiological levels significantly reduced IS-induced cell death but restoring other major ion species (such as K^+, Na^+ and Ca^{2+}) to normal physiological levels dramatically exacerbated IS-induced cell death (Yao et al. 2007b). These data suggested to us that Cl^- homeostasis played a predominant role in cell death in the ischemic penumbra.

4,4'-diisothio-cyanostilbene-2,2'-disulfonic acid (DIDS) is an organic anion that is routinely used as an inhibitor of anion exchangers and Cl^- channels (Wangemann et al. 1986; Romero et al. 1997). However, recent studies have demonstrated that DIDS inhibits cell death induced in human lymphoid U937 and epithelial Hela cells (Maeno et al. 2000), cultured cerebellar granule cells , cortical neurons and glial cells (Himi et al. 2002; Tauskela et al. 2003; Yao et al. 2007b; Xue et al. 2008). Furthermore, in an in vivo transient forebrain ischemia model, Inoue et al have shown that DIDS can attenuate delayed neuronal death in hippocampal CA1 neurons (Inoue et al. 2007). In searching for the mechanisms underlying the dysregulation of Cl^- homeostasis which can lead to cell injury and death, we tested some pharmacologic agents, including DIDS, that can potentially affect flux regulation of Cl^- and other ionic species. Unlike a number of agents that we used, DIDS dose-dependently, protected against IS-induced cell death in astrocytes and neurons (Yao et al. 2007b; Xue et al. 2008). In this work, we extend our observations by examining the mechanisms that underlie the effect of DIDS on penumbral tissue. Using gene expression profile analysis, we show that IS significantly up-regulated the expression of Toll-like receptor 2 (TLR2, an innate immunity-related gene) and its downstream IL-1β (a pro-inflammatory cytokine) and that DIDS inhibited this up-regulation and remarkably protected neurons after IS exposure.

Materials and Methods

Organotypic slice cultures

Animal use was approved by the Institutional Animal Care and Use Committee of the University of California, San Diego. TLR2-deficient mice and C57BL/6J mice were purchased from Jackson Laboratory (Bar Harbor, Me). Hippocampal slice cultures were prepared and maintained as described previously (Yao et al. 2007a). Briefly, mice (6–8 day old) were anesthetized with halothane. The brains were removed and transferred quickly into an ice-cold dissection medium (Gey's balanced salt solution supplemented with D-glucose

6.5 mg/ml). Hippocampi were dissected out and cut transversely into slices of 300 μm each using a Vibratome™ 800-McIllwain Tissue Chopper (Vibratome, St. Louis, MO). Slices were carefully transferred into the 30 mm Millicell-CM tissue culture inserts (Millipore™, Bedford, MA) and placed in 35 mm culture dishes (4–6 slices per insert). Culture media contained Basal Eagle Medium (50%), Earle's Balanced Salt Solution (25%), horse serum (25%) and L-Glutamine (1 mM). Before use, the above culture medium was supplemented with 50U/ml penicillin/streptomycin and 36mM glucose. Cultures were maintained in a 5% CO_2, 37°C incubator for 14 days before experiments were performed. Culture medium was half-replaced on the second day after plating and twice a week thereafter until the day of treatment. Chemicals used in the above media were obtained from Invitrogen (Grand Island, NY) or Sigma (St. Louis, MO).

Quantification of cell death

Cell damage was assessed with propidium iodide (PI) which enters damaged cells and intercalates into DNA with enhanced fluorescence. Five μg/ml PI was added into the culture medium 24 hrs before any treatment and kept at the same concentration throughout the experiment. PI fluorescence was observed on an inverted microscope equipped with a rhodamine filter set that has a 540–552nm band-pass filter for excitation and a 590nm long-pass filter for emission (Zeiss Axiovert 200M microscope, Zeiss, Yena, Germany). An F-Fluar 5X objective (Zeiss, Yena, Germany) and the attached 12 bit CCD camera (C4742, Hamamatsu, Herrsching, Germany) were routinely used for image acquisition. The light source, microscope and camera were controlled by a computer (Universal Imaging Corporation, Downington, PA). For data collection, the parameters of the microscope such as light intensity for excitation, exposure time, camera gain etc., were kept constant. Images were acquired and analyzed with MetaFluor imaging-processing software (Universal Imaging Corporation, Downington, PA). The fluorescence intensity was measured offline in the hippocampal CA1 region, as detailed in our previous paper (Yao et al. 2007a) and the mean fluorescence intensity was expressed as mean fluorescence intensity (MFI).

Experimental conditions

a) ACSF balanced with 5% CO_2 + room air. ACSF contained (in mM): NaCl 129, KCl 5, $CaCl_2$ 1.3, $MgCl_2$ 1.5, $NaHCO_3$ 21, glucose 10. The osmolarity was 315 mOSM and pH was 7.4; b) IS balanced with 15% CO_2 + 1.5% O_2 + N_2. IS contained (in mM): NaCl 47, KCl 29, K-Gluconate 35, $MgCl_2$ 1.5, $CaCl_2$ 0.13, $NaHCO_3$ 4, Glucose 3 and Glutamate 0.1. The osmolarity was adjusted to 315–320 mOSM with sucrose and pH was 6.4. All of the above chemicals were obtained from Sigma.

Micro-array hybridization and analysis

Total RNA was extracted from pooled slices by an RNeasy Mini kit (Qiagen) according to the manufacturer's instructions. The RNA quality was assessed using Agilent 2100 bioanalyzer (Agilent Technologies). The Bioanalyzer determines the integrity/purity of the RNA samples and permits the screening of total RNA sample degradation and ribosomal RNA contamination. We have chosen 2 hrs of IS treatment as a time point for microarray analysis since significant RNA degradation occurred when slices were treated with IS for longer duration (data not shown). One hundred nanograms of mRNA from slices incubated with ACSF, IS or IS+DIDS were analyzed on Illumina Sentrix Mouse-6 Expression BeadChip (Illumina, San Diego, CA). Triplicates were run for each condition with independently isolated RNA from independent experiments. The raw intensity values obtained from the scanned array images were compiled using the proprietary BeadStudio v1.5.1.3 software and imported into VAMPIRE which uses a Bayesian approach to identify altered genes between different treatment groups (Zhang et al. 2006). The data set from microarray analyses can be traced under the Gene Expression Omnibus (GEO) series access

number GSE12426 in the National Center for Biotechnology Information GEO database (http://www.ncbi.nlm.nih.gov/geo). We compared the gene expression profile in slices treated with or without IS, and slices treated with IS in the absence or presence of DIDS. A Bonferroni multiple testing correction ($\alpha_{Bonf} < 0.05$) was applied to identify only those genes with the most robust changes. Microarray data were further analyzed using Ingenuity Pathways Analysis (Ingenuity Systems, www.ingenuity.com). Ingenuity Pathway Analysis is a web-based application that enables the discovery, visualization, and exploration of therapeutically relevant gene networks. It was used to generate specific biological networks in a subpopulation of IS-up-regulated genes that were suppressed by DIDS. This group of genes was mapped to its corresponding gene object in the Ingenuity Pathways Knowledge Base via the Refseq number. These genes, called Focus Genes, were then used as the starting point to generate biological networks. To build the relevant networks, the application queried the Ingenuity Pathways Knowledge Base for interactions between Focus Genes and all other gene objects in the knowledge base and generated a set of networks with a network size of ~35 genes. A significant score was computed for each network according to the size of the network and the fit of the uploaded set of significant genes. This score is based on a right-tailed Fisher's exact test identifying networks that have significantly more focus genes than expected by chance. The biological functions were calculated and assigned to each network by using the Ingenuity Pathways Knowledge Base. The biological functions assigned to each network are ranked according to the significance of that biological function to the network. Again, a right-tailed Fisher's exact test is used to calculate a *P* value determining how likely it is that genes from that network belong to a specific biological function.

Quantitative real-time PCR

Real-time quantitative RT-PCR was performed as previously described (Chu et al. 2004). Briefly, reverse transcription was performed using 200 ng of total RNA and Oligo$(dT)_{20}$ in a 20-μl reaction according to the manufacturer's protocol (Invitrogen). The mouse TLR2 and other gene primers were designed using the Primer 3 software (Rozen and Skaletsky 2000). Real-time PCR was performed on the 7500 Fast Real Time PCR System (Applied Biosystems). The 20-μl PCR contained 100 ng of cDNA, 200 nM primers and other components from the Power SYBR Green PCR Master Mix solution (Applied Biosystems). Housekeeping gene β-actin was evaluated using the same PCR protocol as TLR2. The specificity of PCR for target genes (cDNA) was verified by no signal in no-template controls or reverse transcription (−) samples. The threshold cycle was recorded for each sample to reflect the mRNA expression levels. The comparative threshold cycle method was used to demonstrate the relative expression level of TLR2 and other candidate mRNA as previously reported (Chu et al. 2004). Primers used were as follows: TLR2: (110bp) Left: CTCCCACTTCAGGCTCTTTG; Right: TTATCTTGCGCAGTTTGCAG; IL-1β: (133bp) Left: CCCAAGCAATACCCAAAGAA; Right: GCTTGTGCTCTGCTTGTGAG; β-Actin: (138bp) Left: GATCTGGCACCACACCTTCT; Right: GGGGTGTTGAAGGTCTCAAA.

Western blot

Control and treated slices were recovered separately at the required times and proteins were extracted with HEPES buffer pH 7.5 (200mM Mannitol, 80mM HEPES, 41mM KOH, 1 tablet/50ml of complete protease inhibitor tablets [Roche Diagnostics, Mannheim, Germany], and 230μM OMSF, pH 7.5). Sample protein concentration was determined using the BioRad DC Protein Assay Kit. 40μg proteins per sample were resolved on 10% precast NuPAGE Bis-Tris gels (Invitrogen, Carlsbad, CA) and electrotransferred onto polyvinylidene difluoride membranes (Immobilin-P, Millipore, Bedford, MA). Membranes were then blocked in 5% nonfat dry milk (Carnation, Nestle Food, Glendale, CA) in PBS with 0.1% Tween 20 (MPBST, Sigma) for 1h, and stained with primary antibody (rabbit

anti-TLR2, Cell Signalling, 1/1000; mouse goat anti-actin, Santa Cruz, 1/500) and incubated overnight at 4°C. Membranes were then washed and incubated with secondary antibodies (peroxidase goat anti-rabbit 1/2000 and peroxidase rabbit anti-goat 1/2000, respectively-Zymed Laboratories) for 1.5h at room temperature, then washed and stained with ECL kit. Scanning densitometry of immunoblot films was performed on a Personal Densitometer SI scanner (Molecular Dynamics, Sunnyvale, CA) and analyzed with the aid of ImageQuant image analysis software (Molecular Dynamics, Sunnyvale, CA). Densitometry measurements of Western blots from each experimental group were obtained, and absolute values were normalized to actin.

Data analysis

Data are expressed as means ± SD. Statistically significant differences were determined by a two-way RM ANOVA followed by Bonferroni's post-test unless otherwise indicated, using Prizm (GraphPad, San Diego CA). The criterion for statistical significance is a p value of <0.05. Microarray data were analyzed by Vampire (http://genome.ucsd.edu/microarray, (Zhang et al. 2006)), a statistical package designed to specifically account for the expression-dependent variability in microarray data. The significance threshold was set at $P < 0.05$ after Bonferroni correction for multiple comparisons. The statistical significance of other differences between knockout and wild-type mice was determined with Student's unpaired t-test (2 tailed).

Results

DIDS protection against IS-induced neuronal cell death

IS treatment caused a significant increase in PI uptake in hippocampal slices (Fig. 1A top row). For example, following 24 hrs of IS treatment, the mean PI uptake in the CA1 region increased from baseline (72±25) to 1206±530 (n=12), which was significantly greater than that in ACSF (from baseline (83±25) to 250±92, n=12, p<0.05) (Fig. 1B). With the addition of 400 μM DIDS, IS-induced PI uptake increased very little (Fig. 1A bottom row). In the CA1 region, for example, the PI uptake increased from a mean baseline of 76±13 to 88±16 (n=12), which is a remarkable prevention of an increase in PI uptake when compared to the PI uptake after 24 hrs of IS treatment (1206±530, n=12, p<0.05). The effects of different concentrations of DIDS (1, 10, 100, 1000, 4000 μM) were also tested during IS exposure. Twelve slices from each IS-treated group (with different concentrations of DIDS added) were used to measure PI uptake in the CA1 region. Fitting of the data yielded a dose-response curve (sigmoidal curve) as shown in Fig. 1C. The derived IC_{50} was ~26±1 μM (n=12, Fig. 1C).

Response time window and reversibility of DIDS effect

To determine the time window during which the 'DIDS-blockable' mechanisms exerted their protective effect, we examined the time points (when DIDS was added after IS treatment) at which DIDS can significantly attenuate cell death. DIDS (400 μM) was added at 0, 2, 4, 6 hrs *after* the onset of IS exposure. Figure 2A illustrates the mean PI uptake in the CA1 region, measured following 24 hrs of IS treatment. The increase in PI uptake was significantly attenuated by DIDS added at every time point after the onset of IS treatment. For example, the PI uptake was significantly lower (141±22, n=12, p<0.001) than what it would have been (1206±530, n=12) after 24 hrs of IS treatment if DIDS was added even after 6 hrs of the onset of IS exposure (Fig. 2A).

In another set of experiments, DIDS (400 μM) was added at the onset of IS exposure but was withdrawn after 24 hrs of treatment and the PI fluorescence was measured after 24 hrs of DIDS withdrawal. Figure 2B shows that after the withdrawal of DIDS, a 24-hr IS

exposure significantly increased the mean PI uptake in the CA1 region from 88±16 (n=12) to 940±281 (n=12, $p<0.001$), indicating that IS can still induce injury in these slices. Therefore, DIDS blockade of IS-induced injury is reversible.

Gene expression after IS and DIDS treatments

In order to probe for the basis of DIDS effect and the potential mechanisms of DIDS protection, we studied gene expression profiles in slices using Illumina Mouse 6 chips. The fold change and p value of the differentially expressed genes were obtained by comparing IS-treated slices with control (ACSF) using the VAMPIRE statistical framework (Hsiao et al. 2005). This analysis identified 97 genes that were significantly up-regulated and 104 genes that were significantly down-regulated following the first 2 hrs of IS treatment (Fig. 3Ca and Cb top, respectively). Among these differentially expressed genes, a majority were altered by 1.5–3.5 fold while others were changed by 3.5–38 fold (Fig. 3A). We also studied the effect of DIDS on the IS-induced changes of gene expression by comparing IS+DIDS-treated slices with the IS-treated ones. Our data showed that 17 genes were up-regulated while 195 genes were down-regulated by DIDS in IS-treated slices (Fig. 3Ca and Cb, bottom). Most of the altered genes were within 1.5–3.5 fold change and a small group of genes were changed by 3.5–67 fold (Fig. 3B). It is clear that, in the presence of DIDS, a majority of the differentially expressed genes are down-regulated genes. Among these down-regulated genes, 50 were up-regulated by IS itself (Fig. 3Cc, Table 1). These 50 genes represented the biggest group of genes commonly regulated by both IS and DIDS (Fig. 3C).

To gain insight into the interrelationships among these 50 differentially expressed genes, we applied network-based analysis through the Ingenuity Pathways Knowledge Base (IPA) (Calvano et al. 2005). Among these 50 genes, 32 were eligible for network analysis and a total of 6 regulatory networks were linked to DIDS protection of IS-induced cell death. The top 12 functional categories of the genes (whose translation state was affected by IS and DIDS) associated with all 6 networks are shown in Fig. 4. Cellular movement, hematological system development and function, immune and lymphatic system development and function, tissue morphology and immune response were among them. The top two networks with an IPA score of 58 and 9 respectively (indicating a less than 10^{-58} or 10^{-9} chance that the genes in the network are associated together solely due to random events), are listed in table 2. There are 35 molecules in this particular network (based on the Ingenuity's knowledge base) and 22 of them are up-regulated (bolded in Table 2) by IS and are suppressed with DIDS. Genes that are closely related to innate immunity and inflammation such as TLR2, CCRL2 CD14, IL-1β, IL-1α and TNF-α are among these differentially expressed genes. Therefore, these IS-up-regulated genes, which are closely associated with immune response and inflammation are suppressed by DIDS and this reversal of alterations of gene expression could be, we argued, potentially important in the reduction of cell death seen with DIDS. Interestingly and as expected, the increased expression of cytokines (e.g., IL-1β, IL-1α and TNF-α) was associated with a TLR2 up-regulation in our microarrays. We hypothesized therefore that the activation of this immune cascade was responsible, at least in part, to the cell death seen after IS treatment.

IL-1β expression and IS-induced cell death

To confirm that IL-1β gene expression was altered during IS exposure, we performed qRT-PCR experiments. In control slices, there was little detectable IL-1β mRNA while a 2-hr IS treatment induced a nearly 400 fold increase in IL-1β transcript. This huge increase in IL-1β gene expression was abolished in the presence of DIDS (Fig. 5A). Therefore, in response to IS or IS+DIDS, the differential IL-1β gene expression was consistent with the microarray analysis results, although the amplitude of the change was not the same. To examine whether the increased IL-1β in IS-treated slices is deleterious, we tested the effect of an IL-1

receptor antagonist (IL-1ra, with a series of concentrations: 10^{-7}, 10^{-6}, 10^{-5} and 10^{-4} g/ml) on IS-induced cell death in hippocampal slices. Our data showed that, with the highest concentration (10^{-4} g/ml), IL-1ra significantly attenuated the PI uptake in IS-treated slices (Fig. 5B). To confirm the involvement of IL-1β in the IS-induced cell death, we also examined the effect of IL-1β neutralizing antibody (IL-1β Ab) on IS-induced PI uptake in these slices. Our data showed that IL-1β Ab (3×10^{-5} g/ml) significantly attenuated IS-induced cell damage in slices (Fig. 5C).

IS-induced IL-1β expression in TLR2$^{-/-}$ slices

To determine if the enhanced IL-1β gene expression in IS-treated slices resulted from a change in TLR2 expression, we performed qRT-PCR experiments and confirmed that IS elicited more than 8 fold increase in TLR2 transcript while this increase was eliminated by DIDS (Fig. 6A). These results were consistent with those from microarray analysis. Western blot analysis (n=3) showed a change in TLR2 protein level paralleling the change in mRNA. The amount of TLR2 protein doubled after a 2 hr-incubation with IS, and then decreased by half relative to IS after 2h treatment with DIDS. A similar change was observed after 8 hr-treatment. Therefore, both IS and DIDS affect TLR2 at the protein level, implying that pathways downstream of TLR2 are affected as well. (Fig. 6B). The level of IL-1β mRNA in slices derived from TLR2$^{-/-}$ mice and their wild type (WT) counterparts was also examined. As shown in figure 6C, IS induced little change in IL-1β mRNA in TLR2$^{-/-}$ slices (Average 5–7 fold, n=6) in comparison with WT (~400 fold, n=6 $p<0.001$), suggesting that TLR2 is imposing a change in IL-1β expression in the cascade leading to IS-induced cell death.

IS-induced cell death is remarkably attenuated in TLR2$^{-/-}$ slices

To prove the involvement of TLR2 in the IS-induced cell death, we examined the PI uptake in hippocampal slices derived from TLR2$^{-/-}$ mice and their WT counterparts. Figure 7A illustrates the change in PI fluorescence in WT and TLR2$^{-/-}$ slices following IS treatment. Pseudocolor images demonstrate that in response to IS, PI fluorescence increased over time in CA1, CA3, DG and astrocyte-rich areas (ARA) in slices from both WT and TLR2$^{-/-}$ mice, but with a much reduced PI uptake in the latter. Figure 7B represents the time course of PI uptake in the CA1 regions from both WT and TLR2$^{-/-}$ slices. Compared with WT slices, PI uptake in TLR2$^{-/-}$ slices was significantly lower after 8, 12 and 24 hrs of IS treatment (n=36 for each group. ***: $p<0.001$, *: $p<0.05$).

Discussion

In this work, we provide compelling evidence showing that DIDS exerts its protective effect by suppressing TLR2-mediated signaling that is augmented during simulated ischemia. Our IS model mimics the injury of the hypo-perfused penumbral cells that are frequently challenged by the infarct core milieu during stroke. IS seems to up-regulate TLR2 expression (at both mRNA and protein level) and this causes an augmentation of TLR2 signaling and an up-regulation of IL-1β in hippocampal slices. Our data clearly demonstrate that excessive amount of IL-1β is deleterious to neuronal cells and a blockade of this cytokine can prevent injury. DIDS blocks the up-regulation of TLR2 induced by IS and eliminates the activation of IL-1β and the resulting cell death.

Increasing evidence has suggested that DIDS can act as a protectant in a variety of experimental preparations. For example, DIDS has been shown to inhibit cell death induced by apoptotic factors and simulated ischemic conditions in in vitro preparations (Maeno et al. 2000; Himi et al. 2002; Tauskela et al. 2003; Yao et al. 2007b; Xue et al. 2008). The protective effect of DIDS has also been observed in an in vivo transient forebrain ischemia

model in which DIDS attenuated delayed neuronal death in hippocampal CA1 neurons (Inoue et al. 2007). In agreement with these findings, our data demonstrate that DIDS can markedly protect cells in hippocampal slices against IS-induced death, suggesting that DIDS can potentially preserve penumbral cells and prevent infarct expansion during focal ischemia. Given that DIDS protection is observed in different cell types and under several different experimental conditions, it is tempting to speculate that DIDS exerts, most likely, a broad and global protection in the CNS.

One of the important contributions of this work is the observation that DIDS suppresses a subpopulation of IS-up-regulated genes and most of these genes are associated with innate immunity (Table 1). Indeed, by analyzing gene pathways, we identified a network of genes which were up-regulated by IS and depressed by DIDS. Furthermore, we used either pharmacologic or genetic tools in our study to prove the involvement of this network of genes and demonstrated their important role in IS-induced cell death in hippocampal slices. This network is closely associated with innate immune responses and the included genes are critical elements in the signaling cascade producing inflammatory cytokines, chemokines and adhesion molecules. These genes included TLR2, CD14, IL-1β and TNF-α. Remarkably, these genes have been found also to be up-regulated in other ischemic injuries or in vivo stroke animal models (Buttini et al. 1994;Liu et al. 1994;Sharp et al. 2000;Bates et al. 2001;Schmidt-Kastner et al. 2002). For example, the TLR2 gene which was up-regulated in vivo in animal stroke models has been shown to exacerbate the outcome of stroke (Lehnardt et al. 2007;Ziegler et al. 2007) and this non-pathogen related action of TLR2 has also been observed in other experimental models (Babcock et al. 2006;Kigerl et al. 2007). In our experiments, TLR2 was significantly up-regulated following 2 hrs of IS exposure, suggesting that a) our IS model closely mimics focal ischemia and the resulting pathology and b) TLR2 plays a rather generalized role in various ischemia models and hence may be an important therapeutic target. Another important gene that is directly linked to the IS-induced cell injury is IL-1β which seems to be a most up-regulated gene among ~46000 genes tested in our IS model.

Previous work has demonstrated that IL-1β is present in the CNS and originates not only from the peripheral immune system but also from an endogenous production by brain-resident cells, including microglia, astrocytes and neurons (Huang et al. 2006). Several pieces of evidence have indicated that excessive amount of pro-inflammatory cytokine IL-1β (produced in the affected brain tissue), can contribute to progressive cell death in the border zone of the ischemic infarct. For example, injection of IL-1β intra-ventricularly or within the striatum exacerbates the outcome of cerebral ischemia while the administration of recombinant interleukin-1 receptor antagonist (IL-1ra), a naturally occurring antagonist of IL-1β, attenuates such injury (Boutin et al. 2001; Gibson et al. 2004). Consistent with these findings are the blockade of IL-1β up-regulation and the reduced cell death in slices derived from $TLR2^{-/-}$ mice or the protection of IL-1ra and neutralizing IL-1β antibody in slices derived from WT mice in our experiments.

We believe that the damaging effect of excessive IL-1β in the ischemic penumbra is likely related to its capability of inducing apoptotic cell death (Tsuboi et al. 1999; Fortunato and Menon 2003; Thornton et al. 2006). Our preliminary data do show a significant shrinkage in IS-treated neurons (Yao and Haddad, unpublished data), one of the sign of apoptotic cell death. Therefore, the protective effect of DIDS may well be explained by the inhibition of apoptotic cell death mechanisms which have been observed in other preparations under different insults (Maeno et al. 2000; Araki et al. 2002; Han et al. 2003).

One of the mechanisms that regulate IL-1β expression at a transcriptional level is through a toll-like receptor-mediated signaling pathway (Verstak et al. 2007). As a group of important

pattern recognition receptors in the mammalian innate immune system, TLRs serve as a first line of defense against invading pathogens. In response to pathogen invasion, TLRs initiate a downstream signaling cascade that leads to the production of pro-inflammatory cytokines, chemokines and adhesion molecules to protect the host. However, over-activation of TLRs has been implicated in ischemia-related pathogenesis. Recent findings have suggested that some members of the TLR family, especially TLR2, not only is expressed in neurons, astrocytes and microglial cells, but plays an important role in neurodegenerative disorders (Nguyen et al. 2002; Konat et al. 2006). Our data have demonstrated that the IS induced up-regulation of IL-1β requires the presence of TLR2, suggesting that the activation of TLR2 up-regulates IL-1β through the TLR2-myeloid differentiation primary response gene (88) (MyD88)-nuclear factor κB (NF-κB)-IL-1β signaling pathway (Verstak et al. 2007). Indeed, both TLR2 and IL-1β are expressed in the brain either in physiological conditions or under ischemic conditions (Buttini et al. 1994; Ziegler et al. 2007). The activation of TLR2 results in the recruitment of cytosolic adaptor molecules (e.g., MyD88) via the cytoplasmic Toll/IL-1R domain, which in turn facilitates the assembly of a signaling complex. Following these events, NF-κB is activated and translocates into the nucleus, and promotes the transcription of genes that encode pro-inflammatory cytokines such as IL-1β.

Besides its pattern recognition function, TLRs are thought to be activated by endogenous ‘danger signals’ released from injured or necrotic cells (Matzinger 2002) and contribute to the initiation of the inflammatory response as well as ischemic cell death. Therefore, TLR2 signaling may act as a bridge between brain injury and neuroinflammation (Huyton et al. 2007). Several molecules released from injured or dead cells have been shown to activate TLRs, including TLR2. For example, heat shock protein 60 and 70, fibronectin and HMGB1 (High Mobility Group B 1) have been found to activate TLR2 during brain injury (Beg 2002). In our experiment, it is not clear what ligand stimulates TLR2 and it is unlikely that the IS-induced cell death is due to a contamination with microbial ligands since no significant injury was detected in our control slices (within 24 hrs of ACSF incubation). Therefore, TLR2 must have been activated by endogenous ligands (s) in IS-treated slices.

It is not clear how DIDS mediates gene expression under ischemic conditions. Since DIDS is a non-specific blocker and has been shown to interfere with a variety of ion channels and transporters (Liu et al. 1998; Hill 1999; Tauskela et al. 2003; Lu and Boron 2007), we speculate that DIDS may indirectly suppress IS-induced changes of gene expression by reducing intracellular ionic disturbances and stabilizing intracellular acid-base homeostasis. On the other hand, it is also likely that DIDS can potentially enter the cells and directly manipulates gene expression processes. Indeed, several line of evidence have indicated that DIDS can penetrate cells through ion channels, endocytosis or transported by certain transporters (Anwer et al. 1988; Wehner et al. 1993; Laver and Bradley 2006). The exact process of DIDS interfering with gene expression deserves further investigation.

Our data suggest that mechanisms other than TLR2-IL-1β-mediated processes may also be involved in the DIDS action since neither the blockade of IL-1β activity nor the lack of TLR2 could protect to the same level as DIDS. We therefore conclude that a) DIDS protects neurons and glia by affecting the Toll-like receptor mediated pathway; b) other (unknown) cellular signaling pathways that have been affected by IS and restored by DIDS may also contribute to the DIDS action; and c) Cl^- homeostasis could be, to some extent, maintained by DIDS . One of the cellular mechanisms that are attributable to the Cl^- homeostasis is GABA-mediated Cl^- flux which could alter the status of cellular excitability depending on the Cl^- reversal potential and lead to cell damage. Nevertheless, our preliminary data (Yao and Haddad, unpublished) suggest that GABA-mediated mechanisms did not play an important role in DIDS protection in IS-induced cell death.

The pleiotropic nature of DIDS action can raise a concern as to whether this compound could be harmful to neurons under conditions other than those that are under investigation here. Although our data (Fig.1B) from brain slices did not suggest a change in PI uptake by DIDS in ACSF, we can not rule out a possible toxic effect of DIDS at cellular and organellar levels. Indeed, disturbances of cellular homeostasis that could be potentially induced by DIDS, such as osmolarity, pH, Cl^- and HCO_3^- could lead to disturbances in cell integrity. Further investigation is needed to address this issue.

In conclusion, we have described a protective effect of DIDS in an in vitro model that simulates cell death in the ischemic penumbra. Our data show that an innate immune cascade is an important mechanism that is elicited with the use of IS and suppressed by DIDS. TLR2 and its downstream signaling pathway could represent an important therapeutic target to attenuate infarct expansion and improve neurologic outcome in acute stroke therapy.

Abbreviations used

IS	ischemic solution
ACSF	artificial cerebral spinal fluid
PI	propidium iodide
DIDS	4,4'-diisothiocyanatostilbene-2,2'-disulfonic acid
TLR2	Toll-like receptor 2
IL-1β	interleukin-1β

Acknowledgments

This project was supported by NIH PO1 HD 32573 and NIH RO1 HL 66237.

References

Anwer MS, Nolan K, Hardison WG. Role of bicarbonate in biliary excretion of diisothiocyanostilbene disulfonate. Am J Physiol. 1988; 255:G713–G722. [PubMed: 2849312]

Araki T, Hayashi M, Watanabe N, Kanuka H, Yoshino J, Miura M, Saruta T. Down-regulation of Mcl-1 by inhibition of the PI3-K/Akt pathway is required for cell shrinkage-dependent cell death. Biochem Biophys Res Commun. 2002; 290:1275–1281. [PubMed: 11812001]

Babcock AA, Wirenfeldt M, Holm T, Nielsen HH, Dissing-Olesen L, Toft-Hansen H, Millward JM, Landmann R, Rivest S, Finsen B, Owens T. Toll-like receptor 2 signaling in response to brain injury: an innate bridge to neuroinflammation. J Neurosci. 2006; 26:12826–12837. [PubMed: 17151286]

Back T, Hemmen T, Schuler OG. Lesion evolution in cerebral ischemia. J Neurol. 2004; 251:388–397. [PubMed: 15083282]

Baird AE, Benfield A, Schlaug G, Siewert B, Lovblad KO, Edelman RR, Warach S. Enlargement of human cerebral ischemic lesion volumes measured by diffusion-weighted magnetic resonance imaging. Ann Neurol. 1997; 41:581–589. [PubMed: 9153519]

Bates S, Read SJ, Harrison DC, Topp S, Morrow R, Gale D, Murdock P, Barone FC, Parsons AA, Gloger IS. Characterisation of gene expression changes following permanent MCAO in the rat using subtractive hybridisation. Brain Res Mol Brain Res. 2001; 93:70–80. [PubMed: 11532340]

Beg AA. Endogenous ligands of Toll-like receptors: implications for regulating inflammatory and immune responses. Trends Immunol. 2002; 23:509–512. [PubMed: 12401394]

Boutin H, LeFeuvre RA, Horai R, Asano M, Iwakura Y, Rothwell NJ. Role of IL-1alpha and IL-1beta in ischemic brain damage. J Neurosci. 2001; 21:5528–5534. [PubMed: 11466424]

Buttini M, Sauter A, Boddeke HW. Induction of interleukin-1 beta mRNA after focal cerebral ischaemia in the rat. Brain Res Mol Brain Res. 1994; 23:126–134. [PubMed: 8028476]

Calvano SE, Xiao W, Richards DR, Felciano RM, Baker HV, Cho RJ, Chen RO, Brownstein BH, Cobb JP, Tschoeke SK, Miller-Graziano C, Moldawer LL, Mindrinos MN, Davis RW, Tompkins RG, Lowry SF. A network-based analysis of systemic inflammation in humans. Nature. 2005; 437:1032–1037. [PubMed: 16136080]

Chu HW, Campbell JA, Rino JG, Harbeck RJ, Martin RJ. Inhaled fluticasone propionate reduces concentration of Mycoplasma pneumoniae, inflammation, and bronchial hyperresponsiveness in lungs of mice. J Infect Dis. 2004; 189:1119–1127. [PubMed: 14999617]

Fisher M. The ischemic penumbra: a new opportunity for neuroprotection. Cerebrovasc Dis. 2006; 21 Suppl 2:64–70. [PubMed: 16651816]

Fisher M, Ratan R. New perspectives on developing acute stroke therapy. Ann Neurol. 2003; 53:10–20. [PubMed: 12509843]

Fortunato SJ, Menon R. IL-1 beta is a better inducer of apoptosis in human fetal membranes than IL-6. Placenta. 2003; 24:922–928. [PubMed: 14580374]

Garcia JH, Yoshida Y, Chen H, Li Y, Zhang ZG, Lian J, Chen S, Chopp M. Progression from ischemic injury to infarct following middle cerebral artery occlusion in the rat. Am J Pathol. 1993; 142:623–635. [PubMed: 8434652]

Gibson RM, Rothwell NJ, Le Feuvre RA. CNS injury: the role of the cytokine IL-1. Vet J. 2004; 168:230–237. [PubMed: 15501140]

Gonzalez RG. Imaging-guided acute ischemic stroke therapy: From "time is brain" to "physiology is brain". AJNR Am J Neuroradiol. 2006; 27:728–735. [PubMed: 16611754]

Han D, Antunes F, Canali R, Rettori D, Cadenas E. Voltage-dependent anion channels control the release of the superoxide anion from mitochondria to cytosol. J Biol Chem. 2003; 278:5557–5563. [PubMed: 12482755]

Hill CE. The anion transport inhibitor DIDS activates a Ba2+-sensitive K+ flux associated with hepatic exocrine secretion. Can J Physiol Pharmacol. 1999; 77:268–275. [PubMed: 10535675]

Himi T, Ishizaki Y, Murota SI. 4,4'-diisothiocyano-2 ,2'-stilbenedisulfonate protects cultured cerebellar granule neurons from death. Life Sci. 2002; 70:1235–1249. [PubMed: 11883702]

Hsiao A, Ideker T, Olefsky JM, Subramaniam S. VAMPIRE microarray suite: a web-based platform for the interpretation of gene expression data. Nucleic Acids Res. 2005; 33:W627–W632. [PubMed: 15980550]

Huang J, Upadhyay UM, Tamargo RJ. Inflammation in stroke and focal cerebral ischemia. Surg Neurol. 2006; 66:232–245. [PubMed: 16935624]

Huyton T, Rossjohn J, Wilce M. Toll-like receptors: structural pieces of a curve-shaped puzzle. Immunol Cell Biol. 2007; 85:406–410. [PubMed: 17607319]

Inoue H, Ohtaki H, Nakamachi T, Shioda S, Okada Y. Anion channel blockers attenuate delayed neuronal cell death induced by transient forebrain ischemia. J Neurosci Res. 2007; 85:1427–1435. [PubMed: 17394260]

Karonen JO, Vanninen RL, Liu Y, Ostergaard L, Kuikka JT, Nuutinen J, Vanninen EJ, Partanen PL, Vainio PA, Korhonen K, Perkio J, Roivainen R, Sivenius J, Aronen HJ. Combined diffusion and perfusion MRI with correlation to single-photon emission CT in acute ischemic stroke. Ischemic penumbra predicts infarct growth. Stroke. 1999; 30:1583–1590. [PubMed: 10436105]

Kigerl KA, Lai W, Rivest S, Hart RP, Satoskar AR, Popovich PG. Toll-like receptor (TLR)-2 and TLR-4 regulate inflammation, gliosis, and myelin sparing after spinal cord injury. J Neurochem. 2007; 102:37–50. [PubMed: 17403033]

Konat GW, Kielian T, Marriott I. The role of Toll-like receptors in CNS response to microbial challenge. J Neurochem. 2006; 99:1–12. [PubMed: 16899072]

Laver DR, Bradley KM. Disulfonic stilbene permeation and block of the anion channel from the sarcoplasmic reticulum of rabbit skeletal muscle. Am J Physiol Cell Physiol. 2006; 290:C1666–C1677. [PubMed: 16421208]

Lehnardt S, Lehmann S, Kaul D, Tschimmel K, Hoffmann O, Cho S, Krueger C, Nitsch R, Meisel A, Weber JR. Toll-like receptor 2 mediates CNS injury in focal cerebral ischemia. J Neuroimmunol. 2007; 190:28–33. [PubMed: 17854911]

Liu J, Lai ZF, Wang XD, Tokutomi N, Nishi K. Inhibition of sodium current by chloride channel blocker 4,4'-diisothiocyanatostilbene-2,2'-disulfonic acid (DIDS) in guinea pig cardiac ventricular cells. J Cardiovasc Pharmacol. 1998; 31:558–567. [PubMed: 9554805]

Liu T, Clark RK, McDonnell PC, Young PR, White RF, Barone FC, Feuerstein GZ. Tumor necrosis factor-alpha expression in ischemic neurons. Stroke. 1994; 25:1481–1488. [PubMed: 8023366]

Lo EH, Moskowitz MA, Jacobs TP. Exciting, radical, suicidal: how brain cells die after stroke. Stroke. 2005; 36:189–192. [PubMed: 15637315]

Lu J, Boron WF. Reversible and irreversible interactions of DIDS with the human electrogenic Na/HCO3 cotransporter NBCe1-A: role of lysines in the KKMIK motif of TM5. Am J Physiol Cell Physiol. 2007; 292:C1787–C1798. [PubMed: 17251325]

Maeno E, Ishizaki Y, Kanaseki T, Hazama A, Okada Y. Normotonic cell shrinkage because of disordered volume regulation is an early prerequisite to apoptosis. Proc Natl Acad Sci U S A. 2000; 97:9487–9492. [PubMed: 10900263]

Matzinger P. The danger model: a renewed sense of self. Science. 2002; 296:301–305. [PubMed: 11951032]

Nguyen MD, Julien JP, Rivest S. Innate immunity: the missing link in neuroprotection and neurodegeneration? Nat Rev Neurosci. 2002; 3:216–227. [PubMed: 11994753]

Parsons MW, Barber PA, Chalk J, Darby DG, Rose S, Desmond PM, Gerraty RP, Tress BM, Wright PM, Donnan GA, Davis SM. Diffusion- and perfusion-weighted MRI response to thrombolysis in stroke. Ann Neurol. 2002; 51:28–37. [PubMed: 11782981]

Romero MF, Hediger MA, Boulpaep EL, Boron WF. Expression cloning and characterization of a renal electrogenic Na+/HCO3− cotransporter. Nature. 1997; 387:409–413. [PubMed: 9163427]

Rozen S, Skaletsky H. Primer3 on the WWW for general users and for biologist programmers. Methods Mol Biol. 2000; 132:365–386. [PubMed: 10547847]

Schmidt-Kastner R, Zhang B, Belayev L, Khoutorova L, Amin R, Busto R, Ginsberg MD. DNA microarray analysis of cortical gene expression during early recirculation after focal brain ischemia in rat. Brain Res Mol Brain Res. 2002; 108:81–93. [PubMed: 12480181]

Sharp FR, Lu A, Tang Y, Millhorn DE. Multiple molecular penumbras after focal cerebral ischemia. J Cereb Blood Flow Metab. 2000; 20:1011–1032. [PubMed: 10908035]

Tauskela JS, Mealing G, Comas T, Brunette E, Monette R, Small DL, Morley P. Protection of cortical neurons against oxygen-glucose deprivation and N-methyl-D-aspartate by DIDS and SITS. Eur J Pharmacol. 2003; 464:17–25. [PubMed: 12600690]

Thornton P, Pinteaux E, Gibson RM, Allan SM, Rothwell NJ. Interleukin-1-induced neurotoxicity is mediated by glia and requires caspase activation and free radical release. J Neurochem. 2006; 98:258–266. [PubMed: 16805812]

Tsuboi M, Kawakami A, Nakashima T, Matsuoka N, Urayama S, Kawabe Y, Fujiyama K, Kiriyama T, Aoyagi T, Maeda K, Eguchi K. Tumor necrosis factor-alpha and interleukin-1beta increase the Fas-mediated apoptosis of human osteoblasts. J Lab Clin Med. 1999; 134:222–231. [PubMed: 10482306]

Verstak B, Hertzog P, Mansell A. Toll-like receptor signalling and the clinical benefits that lie within. Inflamm Res. 2007; 56:1–10. [PubMed: 17334664]

Wangemann P, Wittner M, Di Stefano A, Englert HC, Lang HJ, Schlatter E, Greger R. Cl(−)-channel blockers in the thick ascending limb of the loop of Henle. Structure activity relationship. Pflugers Arch. 1986; 407 Suppl 2:S128–S141. [PubMed: 2434915]

Wehner F, Rosin-Steiner S, Beetz G, Sauer H. The anion transport inhibitor DIDS increases rat hepatocyte K+ conductance via uptake through the bilirubin pathway. J Physiol. 1993; 471:617–635. [PubMed: 8120826]

Xue J, Zhou D, Yao H, Haddad GG. Role of transporters and ion channels in neuronal injury under hypoxia. Am J Physiol Regul Integr Comp Physiol. 2008; 294:R451–R457. [PubMed: 17977915]

Yao H, Shu Y, Wang J, Brinkman BC, Haddad GG. Factors influencing cell fate in the infarct rim. J Neurochem. 2007a; 100:1224–1233. [PubMed: 17217421]

Yao H, Sun X, Gu X, Wang J, Haddad GG. Cell death in an ischemic infarct rim model. J Neurochem. 2007b; 103:1644–1653. [PubMed: 17727626]

Zhang H, Bailey JS, Coss D, Lin B, Tsutsumi R, Lawson MA, Mellon PL, Webster NJ. Activin modulates the transcriptional response of LbetaT2 cells to gonadotropin-releasing hormone and alters cellular proliferation. Mol Endocrinol. 2006; 20:2909–2930. [PubMed: 16772531]

Ziegler G, Harhausen D, Schepers C, Hoffmann O, Rohr C, Prinz V, Konig J, Lehrach H, Nietfeld W, Trendelenburg G. TLR2 has a detrimental role in mouse transient focal cerebral ischemia. Biochem Biophys Res Commun. 2007; 359:574–579. [PubMed: 17548055]

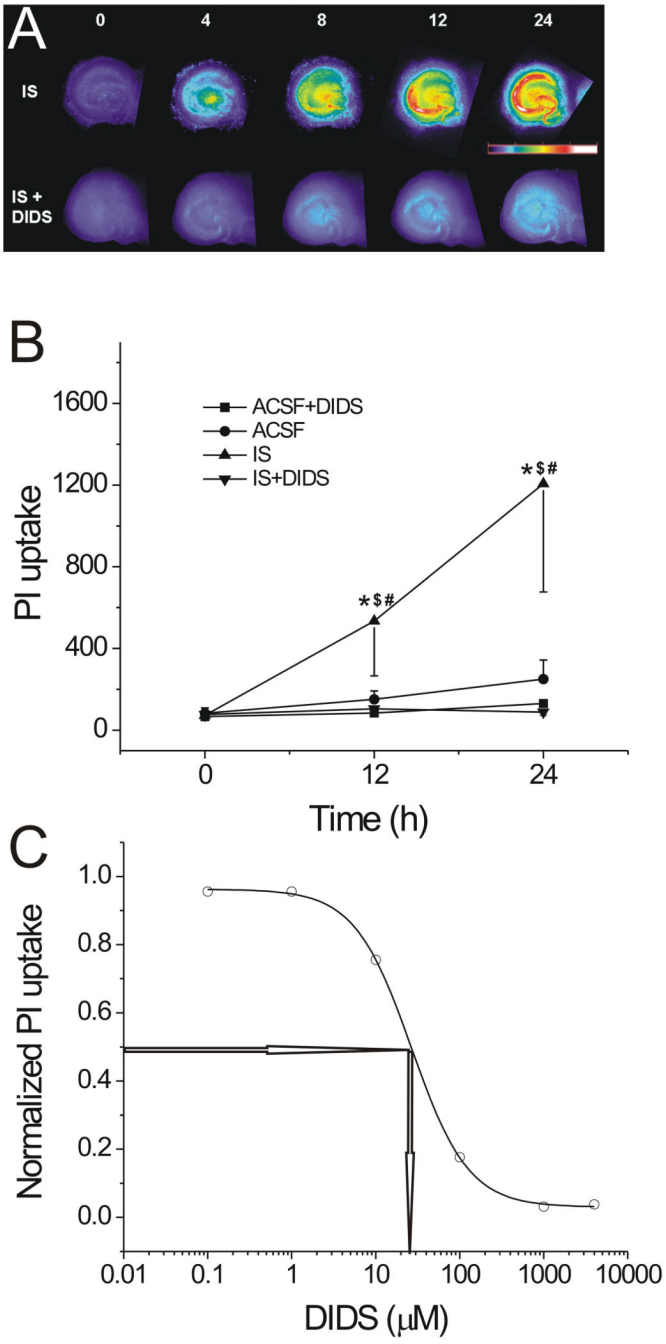

Fig. 1. The effect of DIDS on PI uptake in IS-treated hippocampal slices

A, pseudocolor images showing the IS-induced PI uptake in hippocampal slices at various time points in the absence (top row) or presence (bottom row) of 400 μM DIDS. The numbers above each column represent hours of treatment. The pseudocolor scale is shown on the right middle, with black indicating the least and white the most intense levels of PI fluorescence. B, time courses of mean PI uptake in slices treated with ACSF or IS in the absence or presence of DIDS. *, $, #: $p<0.05$ when compared with ACSF, ACSF+DIDS and IS+DIDS, respectively (n=12 for each group). C, dose-dependence of DIDS effect on IS-induced PI uptake in CA1 region. Dose-response curve of DIDS showing the reduction of IS-induced PI uptake in CA1 region by DIDS. n=12 for each data point. IC_{50}~ 26 μM.

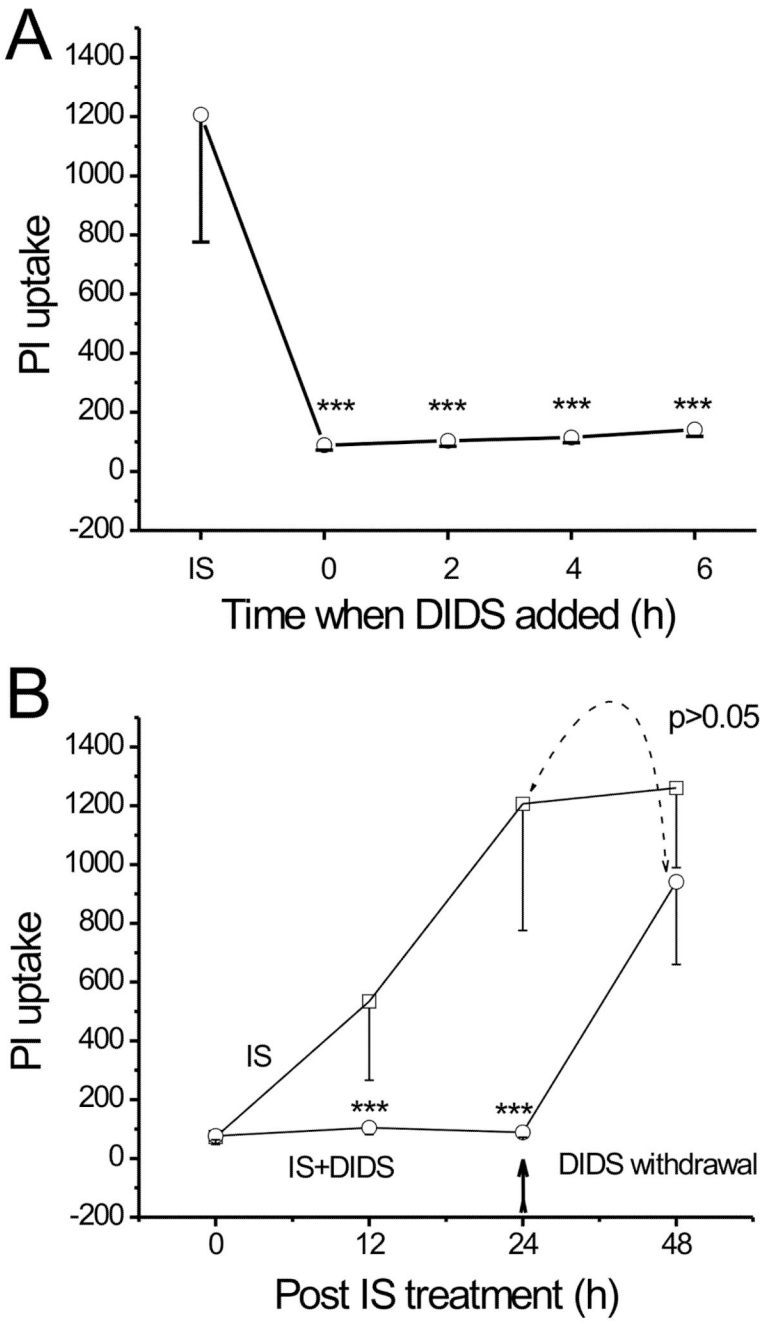

Fig. 2. Protective effect of DIDS is reversible and is effective given after the onset of IS treatment

A, comparison of PI uptake after 24 hrs of IS treatment between control (no DIDS added) and experimental groups treated with DIDS (added at different time points after the onset of IS exposure). The PI uptake in the CA1 region is significantly lower in all groups treated with DIDS (n=12 for each group, ***: $p<0.001$ vs. control), indicating that the protective effect of DIDS is still prominent when applied at 2, 4 or even at 6 hrs after the onset of the IS challenge. B, a comparison of PI uptake after 24 hrs of IS treatment between control (no pre-treatment) and the experimental group pre-treated with IS+DIDS. The two mean PI uptakes compared are indicated by dotted arrow (n=12 for each group, $p>0.05$). ***: $p<0.001$ vs. control at each time point.

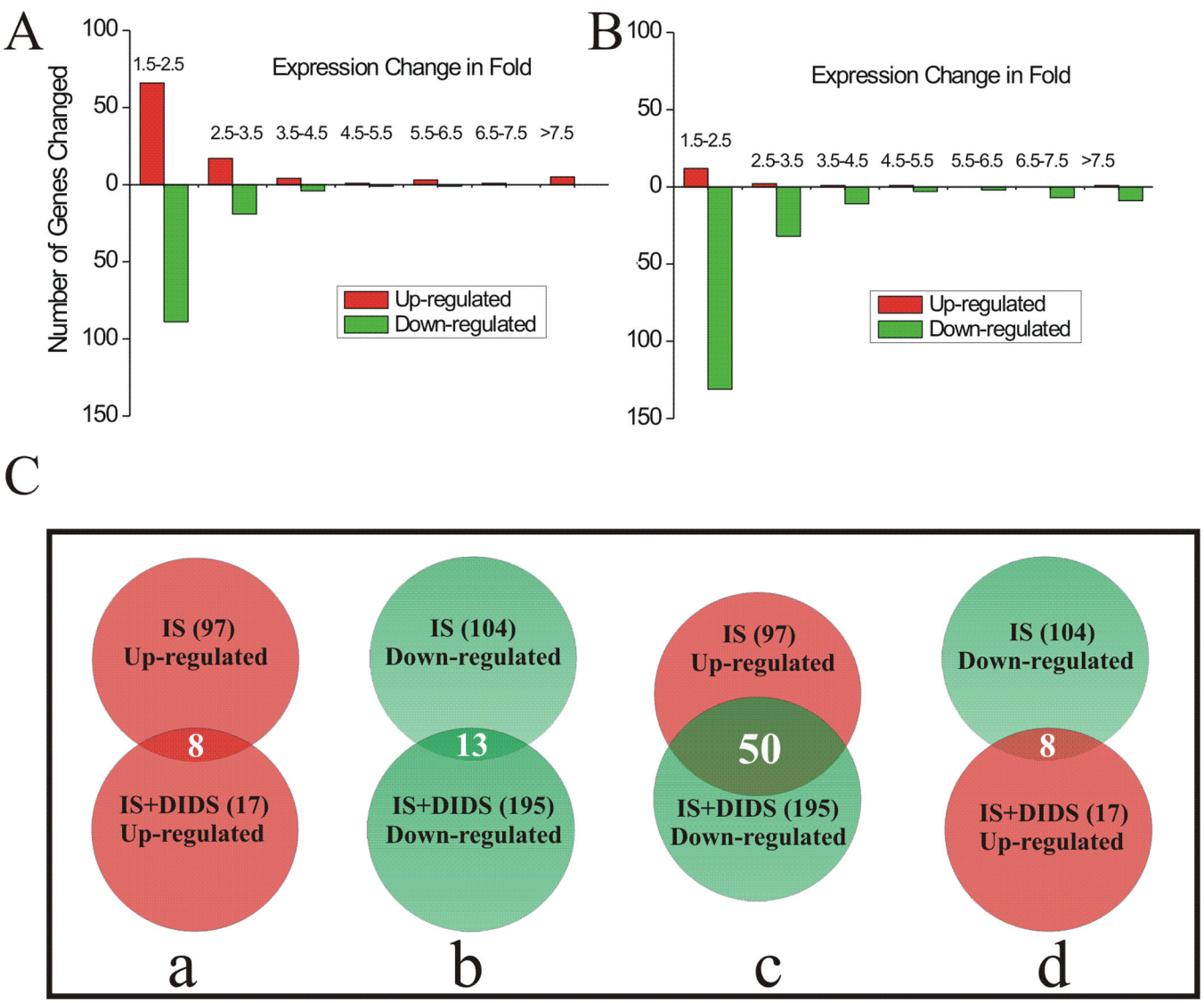

Fig. 3. Microarray results in hippocampal slices following 2 hrs of treatment with IS, IS+DIDS or ACSF

A, distribution of fold changes of gene expression in hippocampal slices following 2 hrs of IS treatment (vs. ACSF group). B, distribution of fold changes of gene expression in hippocampal slices following 2 hrs of IS+DIDS treatment (vs. IS group). Ca–Cd, Venn diagram illustrating the number (shown in each parenthesis) of significantly up-regulated (red) or down-regulated (green) genes following each treatment. The number of genes commonly affected by both treatments is shown without the parenthesis.

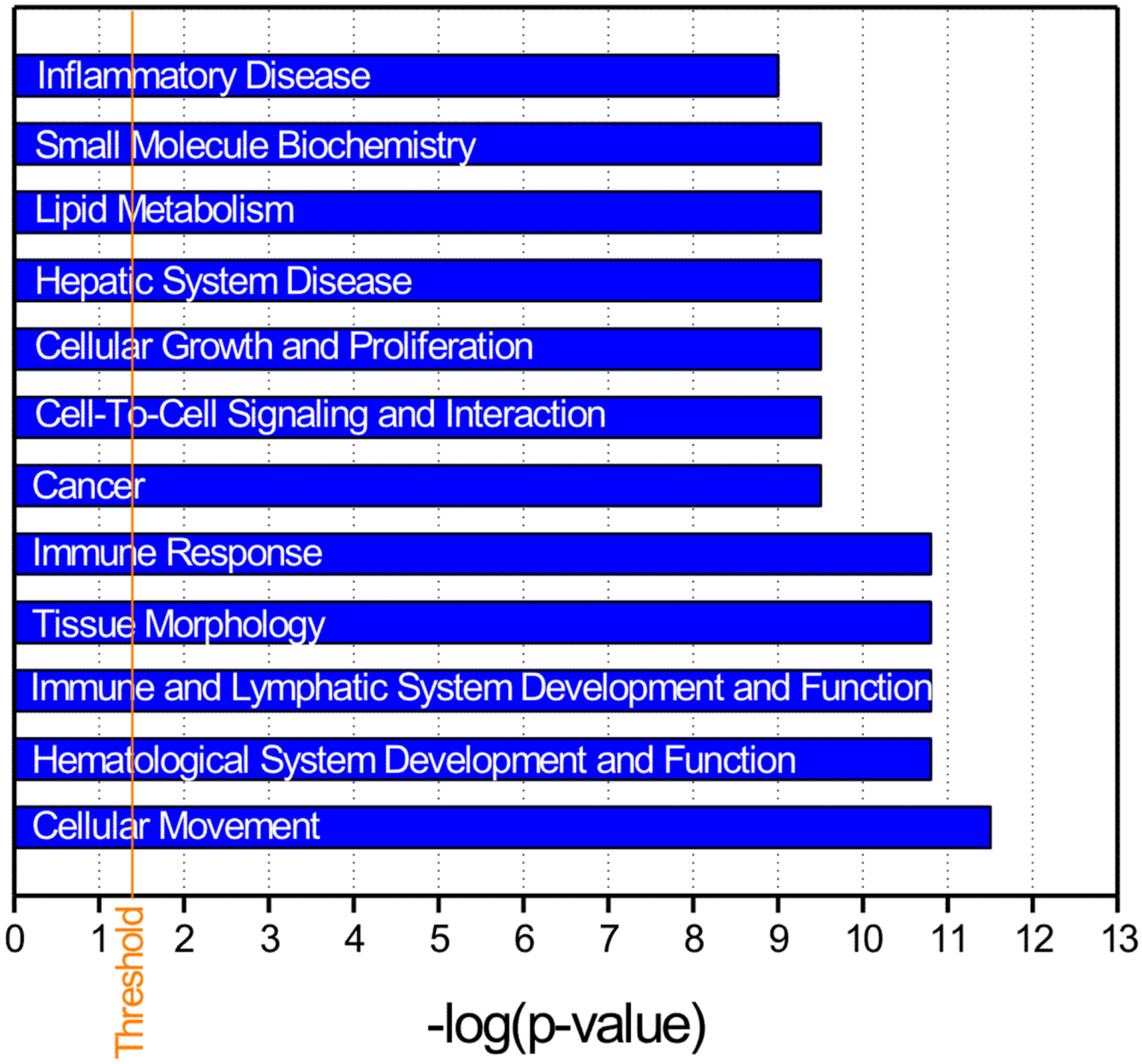

Fig. 4. Pathway analysis of the biological processes underlying DIDS protection in IS-treated hippocampal slices

Bar graph representing 12 top functional categories associated with the networks for the genes that were differentially expressed in the IS-treated slices in both the absence and presence of DIDS. Functional categories are represented in the y-axis. The x-axis designates the significance score (negative log of *p* value). The vertical solid line indicates the significance threshold.

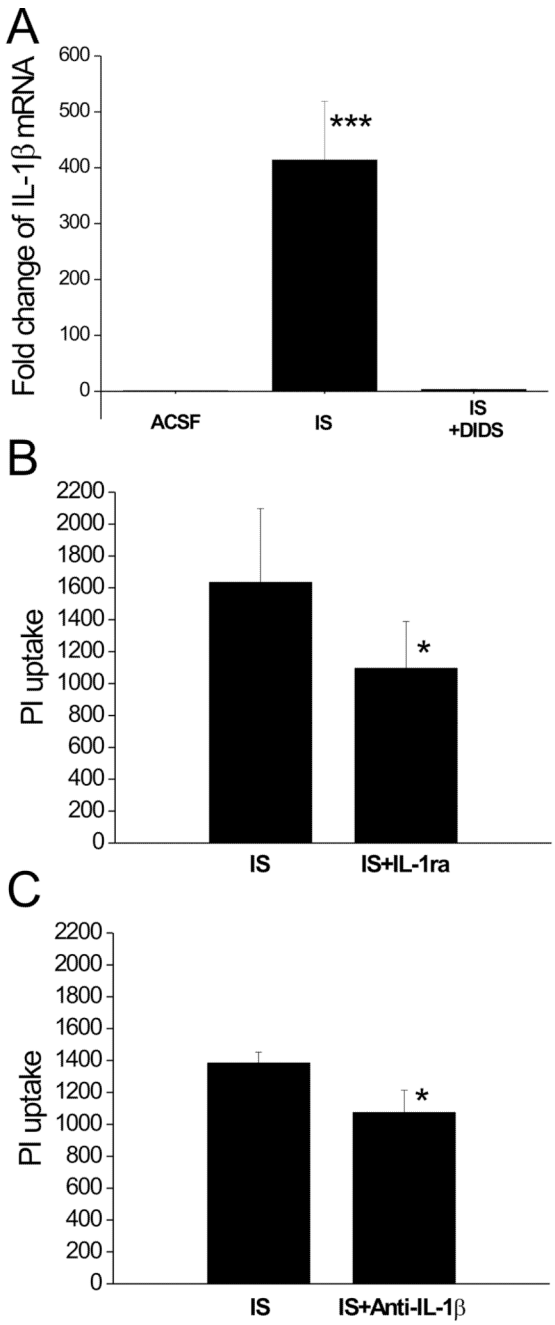

Fig. 5. IL-1β is involved in IS-induced cell death

A, qRT-PCR analysis of IL-1β gene expression in hippocampal slices following 2 hrs of IS, IS+DIDS or ACSF treatment. ***: $p<0.001$ vs. ACSF or IS+DIDS (n=3 for each group). B, the effect of IL-1ra on IS-induced PI uptake in hippocampal CA1 region. Bar graphs showing the PI uptake following 24 hrs of IS treatment with and without 100 μg/ml IL-1ra added. *: $p<0.05$ vs. IS group, n=12 for each group. C, the effect of IL-1β Ab on IS-induced PI uptake in hippocampal CA1 region. Bar graphs showing the PI uptake following 24 hrs of IS treatment with and without the addition of neutralizing antibody directed against IL-1β (15 μg/ml). *: $p<0.05$ vs. IS group, n=6 for each group.

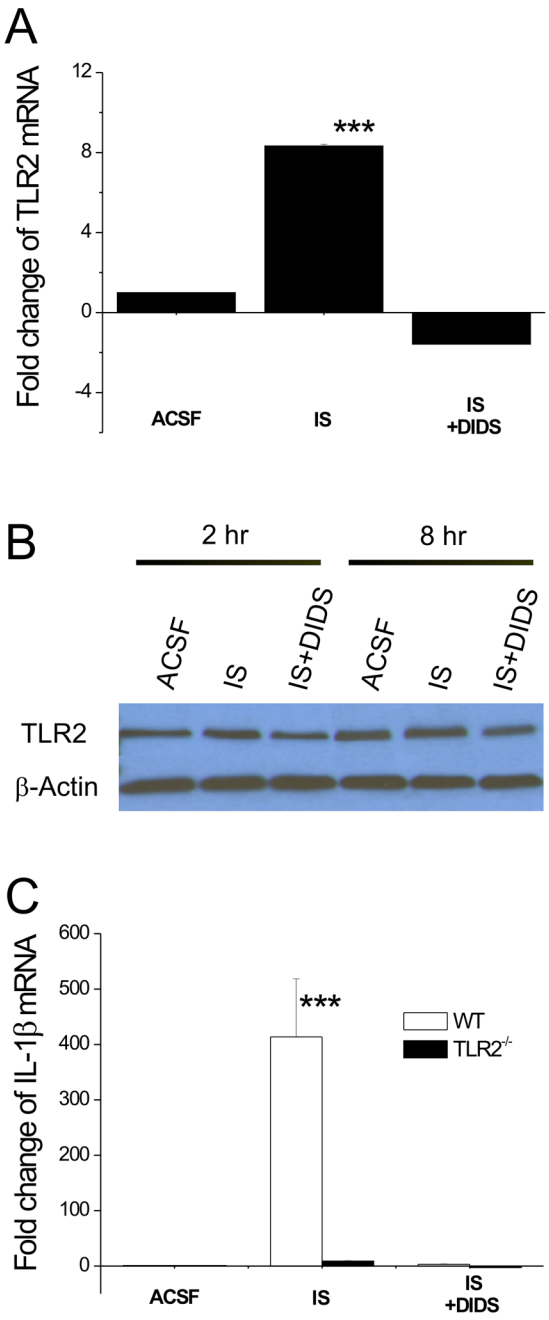

Fig. 6. IS-induced TLR2 up-regulation is upstream of IL-1β expression

A, qRT-PCR analysis of TLR2 gene expression in hippocampal slices following 2 hrs of IS, IS+DIDS or ACSF treatment. n=3 for each group. ***:$p<0.001$ vs. ACSF or IS+DIDS. B, Western blot analysis of TLR2 protein in hippocampal slices following 2 or 8 hrs of IS, IS +DIDS or ACSF treatment. C, qRT-PCR analysis of IL-1β gene expression in $TLR2^{-/-}$ and WT slices following 2 hrs of IS, IS+DIDS or ACSF treatment. ***:$p<0.001$ vs. $TLR2^{-/-}$ group. n=3 for each group.

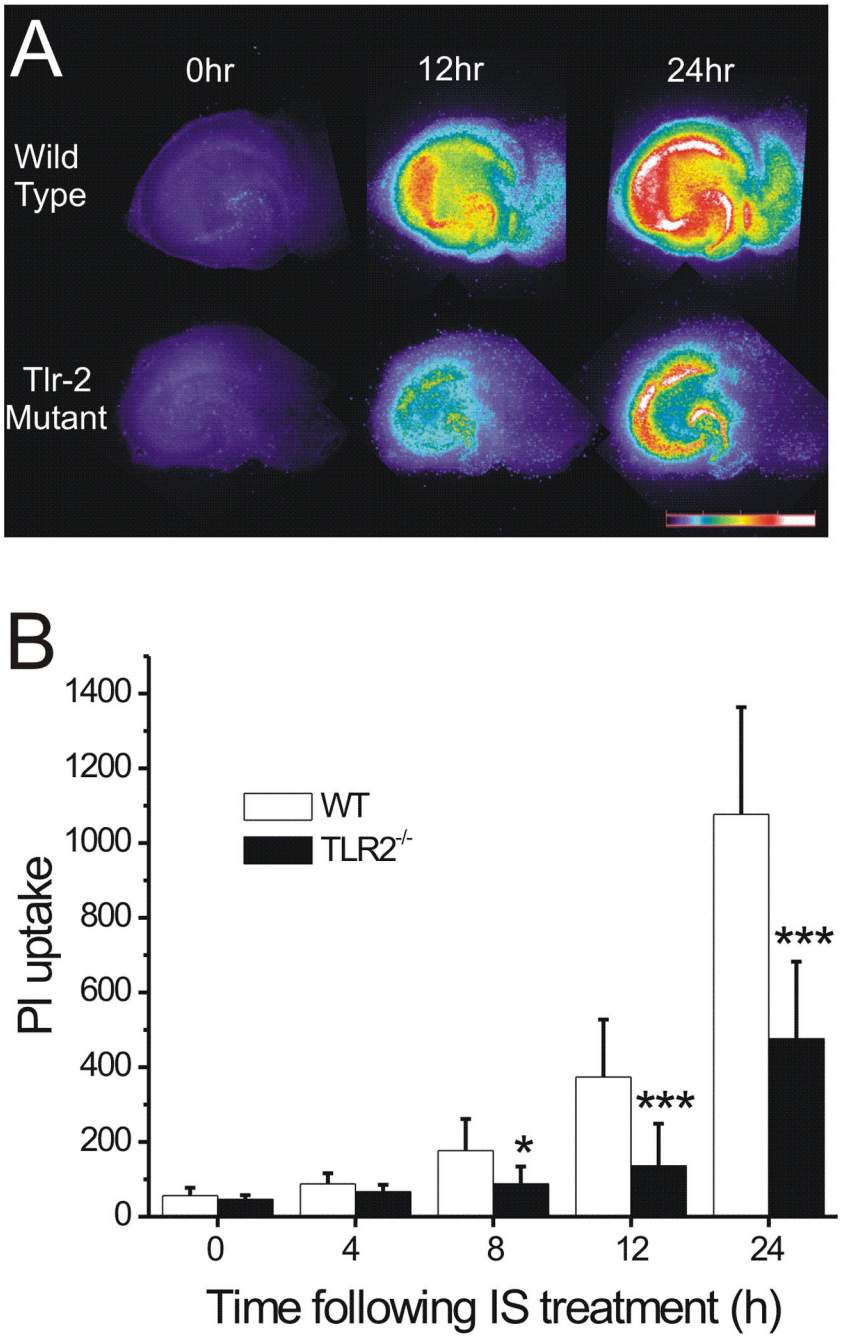

Fig. 7. TLR2 is involved in IS-induced cell death

A, pseudocolor images showing the IS-induced PI uptake at various time points in hippocampal slices derived from WT (top row) or TLR2$^{-/-}$ mice (bottom row). The numbers above each column represent hours of treatment. The pseudocolor scale is shown on the right bottom, with black indicating the least and white the most intense levels of PI fluorescence. B, Time courses of PI uptake following IS treatment. PI uptake calculated from CA1 region was compared between the TLR2$^{-/-}$ and WT slices. *:P<0.05; ***:P<0.001; TLR2$^{-/-}$ vs. WT. n=36 for each group.

Table 1

List of IS-up-regulated genes down-regulated by DIDS

TargetID	Acc	Symbol	IS		IS+DIDS	
			Fold	p Value	Fold	p Value
scl18674.7.1_35-S	NM_008361	Il1b	38.7	5.25E-56	−67.1	3.68E-57
scl054199.2_32-S	NM_017466.3	Ccrl2	19.7	5.03E-53	−27.9	2.53E-54
scl18675.7_38-S	NM_010554	Il1a	8.2	3.06E-37	−10.6	1.03E-30
scl0019225.1_61-S	NM_011198.2	Ptgs2	8.0	2.65E-40	−9.6	5.11E-36
scl53482.9.1_175-S	NM_153553.1	Nxf	7.6	1.32E-39	−5.0	3.98E-28
scl0016175.2_167-S	NM_010554.1	Il1a	7.2	2.49E-34	−9.2	1.50E-27
scl49991.4.1_137-S	NM_013693	Tnf	5.8	4.70E-31	−7.4	4.02E-25
scl46011.5_644-S	XM_127883	Irg1	5.7	1.11E-35	−7.2	2.55E-33
GI_38076622-S	XM_127883.4	Irg1	5.5	2.65E-27	−7.0	3.04E-20
scl37367.3.1_0-S	NM_031252.1	Il23a	4.5	6.59E-19	−4.4	3.76E-11
scl51506.2_48-S	NM_009841.2	Cd14	4.4	3.83E-34	−7.0	1.91E-42
scl0217151.1_189-S	NM_207231.1		3.7	2.87E-27	−5.0	3.32E-28
scl31688.5.1_17-S	NM_008036	Fosb	3.5	2.64E-28	−8.5	6.48E-42
scl39610.3_265-S	NM_007719.1	Ccr7	3.4	9.30E-14	−3.6	2.61E-08
scl020310.4_115-S	NM_009140	Cxcl2	3.4	8.12E-25	−12.3	1.03E-35
scl42750.13_363-S	NM_009396.1	Tnfaip2	3.4	1.54E-20	−5.7	2.00E-19
ri|9630032J03|PX00654H17|AK079342|1822-S	AK079342		3.2	2.43E-20	−2.6	9.30E-12
scl0227929.1_2-S	NM_139200.2	Pscdbp	3.2	1.79E-13	−3.8	4.63E-09

TargetID	Acc	Symbol	IS		IS+DIDS	
			Fold	p Value	Fold	p Value
scl39820.3.1_53-S	NM_013653.1	Ccl5	3.0	1.94E-19	−2.7	1.42E-12
scl016007.2_3-S	NM_010516.1	Cyr61	2.9	2.00E-23	−2.6	7.88E-18
scl52526.2_193-S	NM_016854.1	Ppp1r3c	2.8	1.24E-22	−1.8	3.33E-09
ri|A930011O08|PX00066G06|AK044421|2337-S	AK044421	Rattus norvegicus	2.7	5.89E-16	−3.3	1.58E-13
scl30296.3.272_73-S	NM_023516.3	2310016C08Rik	2.6	4.81E-15	−2.6	3.24E-10
scl0003365.1_125-S			2.6	1.40E-12	−2.4	4.52E-07
scl0003134.1_65-S	M64404		2.5	9.72E-11	−4.5	4.95E-10
scl000798.1_9-S	NM_015811.1	Rgs1	2.4	5.36E-16	−1.9	1.14E-08
scl21413.4_42-S	NM_010516.1	Cyr61	2.3	5.17E-15	−2.9	1.36E-16
scl54837.5.1_4-S	NM_007927.1	Emd	2.3	6.93E-16	−2.3	1.07E-13
scl00105171.1_137-S	NM_178917.2	Arrdc3	2.2	4.87E-16	−2.1	3.87E-13
ri|D130043G23|PX00183B18|AK051380|3224-S	AK051380	cyclin	2.2	6.78E-15	−2.6	4.44E-17
scl51699.17_197-S	NM_013498.1	Crem	2.2	1.00E-12	−2.4	6.36E-11
scl066154.6_169-S	NM_025387.1		2.1	1.26E-14	−1.7	2.79E-08
scl33912.4_501-S	NM_176933.3	Dusp4	2.0	7.13E-12	−2.8	2.07E-14
scl0016600.2_249-S	NM_010637.1	Klf4	2.0	2.06E-11	−6.9	7.69E-27
scl019073.1_109-S	NM_011157.1		2.0	8.30E-13	−1.8	2.22E-09
scl072806.1_8-S			1.9	5.97E-12	−1.9	4.71E-10
scl0002880.1_15-S	NM_007927.1	Emd	1.9	2.89E-11	−2.5	3.01E-17

TargetID	Acc	Symbol	IS		IS+DIDS	
			Fold	p Value	Fold	p Value
scl44840.4_185-S	NM_009856.1	Cd83	1.9	2.99E-11	−6.5	2.63E-40
scl0017294.1_5-S	NM_008590.1	Mest	1.8	1.34E-09	−1.8	6.61E-08
GI_24475922-S	NM_010490.2	Iap	1.8	2.98E-10	−1.7	9.25E-08
scl40250.1.1_66-S			1.8	7.49E-09	−1.9	7.67E-08
scl0012044.1_118-S	NM_009742.2	Bcl2a1a	1.7	1.49E-09	−2.0	3.20E-12
scl0002999.1_1356-S	NM_009373.2	Tgm2	1.7	2.67E-09	−1.7	4.12E-08
ri|D130052N13|PX00184G04|AK051496|2048-S	AK051496		1.7	7.94E-09	−1.7	1.19E-08
scl41377.24.1_22-S	NM_011065.2	Per1	1.7	2.04E-07	−1.9	1.73E-07
scl32816.11.1_261-S	NM_172142.1		1.7	1.94E-07	−2.3	1.72E-10
scl0012045.1_114-S	NM_007534	Bcl2a1b	1.7	7.97E-09	−1.9	4.63E-11
scl0066102.2_212-S	NM_023158.3	Cxcl16	1.7	8.85E-08	−1.8	7.44E-08
scl22018.3_120-S	NM_011905.2	Tlr2	1.7	1.62E-08	−5.9	2.02E-39
GI_38083692-S	XM_355746.1	4732477G22	1.6	3.31E-07	−4.1	2.95E-21
scl0075423.2_59-S	NM_182994.1		1.6	2.89E-07	−1.8	7.31E-08
scl0012047.1_125-S	NM_007536	Bcl2a1d	1.6	1.76E-07	−2.0	2.03E-12
scl6031.1.1_4-S	NM_009166		1.6	2.38E-07	−2.2	3.64E-14

Table 2

The top 2-ranked networks for genes commonly affected by both IS and IS+DIDS

ID	Molecules in Network	Score	Focus Molecules	Top Functions
1	**BCL2A1, CCL5, CCR7, CCRL2, CD14, CD83, CXCL3, CXCL16,** Cyclooxygenase, CYR61, IKK, **IL1,** IL1/IL6/TNF, **IL1A, IL23A, IRG1,** Jnk, **KLF4,** Mmp, NfkB-RelA, Nos, P38 MAPK, **PPP1R3C, PSCDBP, PTGS2, RGS1,** SAA@, Sod, **SORBS1,** Tgf beta, **TGM2, TLR2, TNF, TNFAIP2,** VitaminD3-VDR-RXR	58	22	Cellular Movement, Immune Response, Hematological System Development and Function
2	Akt, Ap1, Caspase, Creb, **CREB3L4**, CREM, Cyclin A, Cyclin E, **DUSP4**, ERK1/2, **FOSB**, Histone h3, Hsp70, **IL1B**, INSRR, Insulin, LDL, Mapk, Nfat, NFkB, p70 S6k, Pdgf, PDGF BB, **PER1**, PI3K, Pka, Pkc(s),PLC, Pld, PLD3, Ras, Ras homolog, RNA polymerase II, STAT5a/b,	9	5	Behavior, Nervous System Development and Function, Cardiovascular Disease